



Existence domains of dust-acoustic solitons and supersolitons

S. K. Maharaj, R. Bharuthram, S. V. Singh, and G. S. Lakhina

Citation: *Physics of Plasmas* (1994-present) **20**, 083705 (2013); doi: 10.1063/1.4818439

View online: <http://dx.doi.org/10.1063/1.4818439>

View Table of Contents: <http://scitation.aip.org/content/aip/journal/pop/20/8?ver=pdfcov>

Published by the [AIP Publishing](#)



Re-register for Table of Content Alerts

Create a profile.



Sign up today!



Existence domains of dust-acoustic solitons and supersolitons

S. K. Maharaj,¹ R. Bharuthram,² S. V. Singh,³ and G. S. Lakhina³

¹South African National Space Agency (SANSA) Space Science, PO Box 32, Hermanus 7200, South Africa

²University of the Western Cape, Robert Sobukwe Road, Bellville 7535, South Africa

³Indian Institute of Geomagnetism, New Panvel, Navi Mumbai 410218, India

(Received 7 June 2013; accepted 28 July 2013; published online 15 August 2013)

Using the Sagdeev potential method, the existence of large amplitude dust-acoustic solitons and supersolitons is investigated in a plasma comprising cold negative dust, adiabatic positive dust, Boltzmann electrons, and non-thermal ions. This model supports the existence of positive potential supersolitons in a certain region in parameter space in addition to regular solitons having negative and positive potentials. The lower Mach number limit for supersolitons coincides with the occurrence of double layers whereas the upper limit is imposed by the constraint that the adiabatic positive dust number density must remain real valued. The upper Mach number limits for negative potential (positive potential) solitons coincide with limiting values of the negative (positive) potential for which the negative (positive) dust number density is real valued. Alternatively, the existence of positive potential solitons can terminate when positive potential double layers occur.

© 2013 AIP Publishing LLC. [<http://dx.doi.org/10.1063/1.4818439>]

I. INTRODUCTION

Dust occurs in a number of astrophysical environments such as planetary rings, planetary nebulae, cometary tails, and also closer to us, in the form of noctilucent clouds in the mesosphere. What makes dusty plasmas unique is that a dust grain is not only very heavy with the mass varying between $10^6 - 10^{12}$ proton masses but also it acquires, most often, a large negative charge with, anywhere between $10^4 - 10^8$ electronic charges. Furthermore, the charge on a dust grain does not remain constant, but it fluctuates which makes dusty plasmas different from the conventional ion-electron plasmas. Because of the smallness of the charge-to-mass ratio of a dust particle in comparison to that for an ion (singly charged) or electron, the dynamics of the massive charged dust occurs on much longer time scales than those associated with the motions of the ions or electrons. A dusty plasma thus supports ultra-low frequency waves, the most notable of which is the dust-acoustic wave (DAW) which has a frequency of only a few Hz. The pressures of the electrons and ions provide the restoring force whereas the inertia required to support the DAW is provided by the dust.

Arbitrary amplitude dust-acoustic solitary structures in multi-component dusty plasmas having fluid or Maxwellian distributed electrons/ions have been studied by Mamun.¹⁻³ A mathematical form for a velocity distribution which has high energy tails in space plasmas and is characterized by the non-thermal parameter α was first proposed by Cairns *et al.*⁴ Ion-acoustic solitary wave structures having both negative and positive potentials were found to be simultaneously supported if a non-thermal velocity distribution is assumed for the electrons ($\alpha = 0.2$) as opposed to only positive potential structures being possible for electrons which are Boltzmann distributed ($\alpha = 0$). Following the study in Ref. 4, there was tremendous theoretical interest in nonlinear DAWs where

the lighter ions or electrons are modelled by a non-thermal velocity distribution. Mamun *et al.*⁵ studied nonlinear DAWs in a system with cold negatively charged dust and non-thermal ions. They found both negative and positive potential dust-acoustic solitary waves. Similarly, the models with adiabatic negative dust and non-thermal ions^{6,7} were also found to support the existence of positive potential dust-acoustic (DA) solitary waves. The positive potential solitary waves in Ref. 7 are limited by the occurrence of positive potential double layers⁸ although the connection between the solitary waves of Ref. 7 and the double layers of Ref. 8 was not pointed out in Ref. 8.

The reasons for the existence of upper limits on the Mach number supporting dust-acoustic solitary waves were discussed in detail by Verheest and Pillay⁹ for a model which is similar to that of Ref. 7 except that the dust is treated as cold. Negative potential solitary wave structures were found to be limited by infinite compression in the number density of the negative dust whereas positive double layers (DLs) were found to occur as upper limits on the Mach number ranges supporting positive potential solitary waves. Reversing the polarity on the dust and the non-thermal species in the model of Ref. 9, Verheest and Pillay¹⁰ showed that negative potential solitary waves are possible. The positive potential solitary wave structures are limited by infinite compression in the positive dust number density whereas the negative potential structures are limited by the occurrence of negative potential DLs. The pattern which emerges from the studies based on the models of Refs. 5-10 is that non-thermal effects of the ions (electrons) drive the existence of DA solitary waves having positive (negative) polarity in dusty plasmas containing only one component of inertial charged dust which is negative (positive). Furthermore, the solitary waves having positive (negative) potential which are driven by non-thermal effects of the ions (electrons) are limited by the occurrence of positive (negative) potential double layers.

Verheest¹¹ discusses the existence of large amplitude dust-acoustic solitary waves in a model composed of both negative and positive cold dust species and inertialess ions and electrons which are both non-thermal. Negative potential solitary waves were found to be limited either by infinite compression in the number density of the negative dust or the occurrence of negative double layers. Positive potential solitary waves were limited only by the onset of infinite positive dust compression since positive double layers were not found. An unusual situation was reported in Refs. 11 and 12 where negative or positive potential solitary waves were still found to occur for Mach number values which exceed that of a double layer (cf. Fig. 8 of Ref. 11 and Fig. 3(b) of Ref. 12). These negative or positive potential solitary wave structures are supersolitons^{13,14} which were limited by infinite compression in the number density of the negative dust (Ref. 11) or ions (Ref. 12). As pointed out in Refs. 13 and 14, supersolitons differ from the regular solitons in that their electric field profiles appear slightly distorted because of the presence of subsidiary extrema in the wings of the bipolar electric field structures. We recall that the existence regions and the factors limiting the existence of supersolitons of the ion-acoustic type are discussed in Ref. 13, whereas dust ion-acoustic supersolitons were investigated in Ref. 14.

Insights into how to identify the regions in parameter space where opposite polarity dust-acoustic solitary waves can coexist was provided by Verheest¹⁵ for a model with negative dust, Boltzmann distributed cool ions, and hot ions which are non-thermal. Coexistence of negative and positive potential solitary waves is found to be supported when the third derivative of the Sagdeev potential at the acoustic speed vanishes.¹⁵

Extending the model of Ref. 16 to include non-thermal effects of the ions, the model composed of cold negative dust, adiabatic positive dust, Boltzmann electrons, and non-thermal ions was adopted by Maharaj *et al.*¹⁷ to investigate the existence regions of large amplitude dust-acoustic solitary waves. In this paper we revisit the model of Ref. 17, but here we perform a more indepth study of the existence regimes of DA solitons by focusing on the upper limits on the admissible soliton Mach number ranges. We recall that in Ref. 17 only the lower limits on the Mach number ranges supporting DA solitons were considered. Here we do not only provide physical insight into why upper limiting values of the Mach number arise for DA solitons, but we also explicitly calculate these upper Mach number limits. Combining the upper Mach number limits found here with the lower limits discussed in Ref. 17, we present here the admissible DA soliton Mach number ranges for much broader regions in parameter space than those found supporting DA solitons in Ref. 17. Our main objective in this study will be to focus on the positive potential soliton structures and to determine to what extent are non-thermal effects of the ions necessary for the existence of *positive* potential solitons for a two-dust model. Here, we show for the first time the existence of dust-acoustic supersolitons and emphasize how the Sagdeev potential and the corresponding electric field profiles of these nonlinear structures differ from those of regular solitons. It is important to mention that throughout the paper we refer solitary and super solitary wave solutions as

solitons and supersolitons. This terminology has been used in many earlier studies, including Verheest *et al.*^{13,14}

In Sec. II we present our model and governing equations. In Sec. III we justify why upper limits arise on the admissible dust-acoustic soliton and supersoliton Mach number ranges found in this paper. Existence regions of dust-acoustic solitons as well as supersolitons are presented and discussed in Sec. IV. Finally, we conclude by presenting a summary of our results in Sec. V.

II. THEORETICAL MODEL AND GOVERNING EQUATIONS

We consider a four component unmagnetized dusty plasma comprising a negatively charged cold dust fluid, a positively charged warm dust fluid, non-thermal ions, and Boltzmann electrons. The ions are assumed to be non-thermal and have a velocity distribution similar to that used for non-thermal electrons in the study by Cairns *et al.*⁴ with the normalized non-thermal ion number density given by

$$n_i = \mu_i(1 + \beta\Psi + \beta\Psi^2)e^{-\Psi}. \quad (1)$$

Here Ψ is the normalized electrostatic potential (with respect to $k_B T_i/e$) and $\beta = 4\alpha/(1 + 3\alpha)$ with α being the ion non-thermal parameter⁴ and $\mu_i = n_{i0}/(Z_{dn}n_{dn0})$ is the normalized equilibrium ion number density. Setting $\alpha = 0$, the expression (1) for the number density of the non-thermal ions reverts to that for Boltzmann ions considered in the model of Mamun.¹⁶

The electrons are in thermal equilibrium at temperature T_e . Their number density in normalized form is given by the Boltzmann expression

$$n_e = \mu_e e^{\sigma\Psi}, \quad (2)$$

where $\sigma = T_i/T_e$ and $\mu_e = n_{e0}/(Z_{dn}n_{dn0})$ is the normalized equilibrium electron number density.

The basic set of equations in normalized form governing the dynamics of the negative and positive dust species as appears in Ref. 17 is given by

$$\frac{\partial n_{dn}}{\partial t} + \frac{\partial(n_{dn}v_{dn})}{\partial x} = 0, \quad (3)$$

$$\frac{\partial v_{dn}}{\partial t} + v_{dn} \frac{\partial v_{dn}}{\partial x} = \frac{\partial\Psi}{\partial x}, \quad (4)$$

$$\frac{\partial n_{dp}}{\partial t} + \frac{\partial(n_{dp}v_{dp})}{\partial x} = 0, \quad (5)$$

$$\frac{\partial v_{dp}}{\partial t} + v_{dp} \frac{\partial v_{dp}}{\partial x} = -\delta \left(\frac{\partial\Psi}{\partial x} + \frac{\sigma_{dp}}{n_{dp}} \frac{\partial P_{dp}}{\partial x} \right), \quad (6)$$

$$\frac{\partial P_{dp}}{\partial t} + v_{dp} \frac{\partial P_{dp}}{\partial x} + 3P_{dp} \frac{\partial v_{dp}}{\partial x} = 0. \quad (7)$$

The system of equations is closed by Poisson's equation which is given by

$$\frac{\partial^2 \Psi}{\partial x^2} = n_{dn} - n_{dp} + \mu_e e^{\sigma \Psi} - \mu_i (1 + \beta \Psi + \beta \Psi^2) e^{-\Psi}. \quad (8)$$

The normalizations we have used are the same as in Ref. 16. The normalized quantity n_{dn} (n_{dp}) denotes the number density of the negative (positive) dust having been normalized by its equilibrium number density n_{dn0} (n_{dp0}), the negative (positive) dust fluid velocity in dimensionless form is denoted by v_{dn} (v_{dp}) having been normalized by $C_{dn} = \sqrt{Z_{dn} k_B T_i / m_{dn}}$, the electrostatic wave potential in dimensionless form is denoted by Ψ having been normalized by $k_B T_i / e$, the normalized pressure of the positive dust fluid is denoted by P_{dp} having been normalized by $n_{dp0} k_B T_{dp}$ where T_{dp} denotes the equilibrium temperature of the positive dust fluid. The ratio of the charge-mass ratios of the positive and negative dust species is given by $\delta = Z_{dp} m_{dn} / Z_{dn} m_{dp}$, $\sigma_{dp} = T_{dp} / (Z_{dp} T_i)$ is the normalized temperature of the positive dust, and $\mu_{dp} = Z_{dp} n_{dp0} / Z_{dn} n_{dn0}$ is the normalized equilibrium positive dust number density. In the definitions above, m_{dn} (m_{dp}) is the mass of the negative (positive) dust grains, and Z_{dn} (Z_{dp}) denotes the number of electrons (positive charges) residing on a negative (positive) dust grain. The temperature of the ions (electrons) is denoted by T_i (T_e), e denotes the magnitude of the electronic charge, and k_B is the Boltzmann constant. Time t is normalized with respect to $\omega_{pn}^{-1} = (m_{dn} / 4\pi Z_{dn}^2 n_{dn0} e^2)^{1/2}$ and spatial variable is normalized by $\lambda_D = (k_B T_i / 4\pi Z_{dn} n_{dn0} e^2)^{1/2}$.

Charge neutrality at equilibrium (in unnormalized form) is assumed, viz.,

$$n_{i0} + Z_{dp} n_{dp0} = n_{e0} + Z_{dn} n_{dn0}, \quad (9)$$

which in normalized form yields

$$\mu_i + \mu_{dp} = \mu_e + 1. \quad (10)$$

Examination of Eq. (10) reveals that our choice of normalizations¹⁶ takes into account the sharing of positive charge

between the positively charged dust and the free positive charge. We have assumed that the equilibrium number density of the negative dust is never zero because our normalizations are with respect to the negative dust. We also assume that the ion number density is never zero since our normalizing acoustic speed C_{dn} is defined in terms of ion pressure (finite value for T_i).

Following the procedure in Ref. 6 to obtain solitary wave solutions, the set of equations (3)–(8) in the stationary frame $\xi = x - Mt$ (where the Mach number M is the velocity of the nonlinear structure normalized with respect to the dust-acoustic speed C_{dn}) yields

$$-M \frac{\partial n_{dn}}{\partial \xi} + \frac{\partial (n_{dn} v_{dn})}{\partial \xi} = 0, \quad (11)$$

$$-M \frac{\partial v_{dn}}{\partial \xi} + v_{dn} \frac{\partial v_{dn}}{\partial \xi} = \frac{\partial \Psi}{\partial \xi}, \quad (12)$$

$$-M \frac{\partial n_{dp}}{\partial \xi} + \frac{\partial (n_{dp} v_{dp})}{\partial \xi} = 0, \quad (13)$$

$$-M \frac{\partial v_{dp}}{\partial \xi} + v_{dp} \frac{\partial v_{dp}}{\partial \xi} = -\delta \left(\frac{\partial \Psi}{\partial \xi} + \frac{\sigma_{dp}}{n_{dp}} \frac{\partial P_{dp}}{\partial \xi} \right), \quad (14)$$

$$-M \frac{\partial P_{dp}}{\partial \xi} + v_{dp} \frac{\partial P_{dp}}{\partial \xi} + 3P_{dp} \frac{\partial v_{dp}}{\partial \xi} = 0, \quad (15)$$

$$\frac{\partial^2 \Psi}{\partial \xi^2} = n_{dn} - n_{dp} + \mu_e e^{\sigma \Psi} - \mu_i (1 + \beta \Psi + \beta \Psi^2) e^{-\Psi}. \quad (16)$$

Using the boundary conditions $n_{dn} \rightarrow 1$, $n_{dp} \rightarrow \mu_{dp}$, $n_e \rightarrow \mu_e$, $n_i \rightarrow \mu_i$, $v_{dn} \rightarrow 0$, $v_{dp} \rightarrow 0$, $P_{dp} \rightarrow 1$, and $\Psi \rightarrow 0$ at $\xi \rightarrow \pm\infty$, we obtain the expressions for the number densities of the cold negative dust and adiabatic positive dust which are given by

$$n_{dn} = \frac{1}{\sqrt{1 + \frac{2\Psi}{M^2}}}, \quad (17)$$

$$n_{dp} = \mu_{dp} \frac{\sqrt{(M^2 + 3\delta\sigma_{dp})}}{\sqrt{6\delta\sigma_{dp}}} \sqrt{\left(1 - \frac{2\delta\Psi}{(M^2 + 3\delta\sigma_{dp})}\right)} - \sqrt{\left(1 - \frac{2\delta\Psi}{(M^2 + 3\delta\sigma_{dp})}\right)^2 - \frac{12\delta\sigma_{dp}M^2}{(M^2 + 3\delta\sigma_{dp})^2}}. \quad (18)$$

If we choose to neglect the pressure of the positive dust fluid ($\sigma_{dp} = 0$), instead of Eq. (18), we have the simpler expression

$$n_{dp} = \frac{\mu_{dp}}{\sqrt{1 - \frac{2\delta\Psi}{M^2}}}. \quad (19)$$

The expressions (17)–(19) are identical to those which were obtained in Ref. 16.

Now putting Eqs. (17) and (18) in Eq. (16), multiplying Eq. (16) by $d\Psi/d\xi$, and after integrating, we finally obtain the energy-integral like equation given by

$$\frac{1}{2} \left(\frac{d\Psi}{d\xi} \right)^2 + V(\Psi) = 0, \quad (20)$$

from which the expression for the Sagdeev potential $V(\psi)$ can be obtained, which, for our model, yields

$$\begin{aligned}
 V(\Psi) = & -M^2 \left[\sqrt{1 + \frac{2\Psi}{M^2}} - 1 \right] + \frac{\mu_{dp} M \sqrt{M^2 + 3\delta\sigma_{dp}}}{\delta\sqrt{2}} \left[\sqrt{1 + \sqrt{1 - \frac{12\delta\sigma_{dp}M^2}{(M^2 + 3\delta\sigma_{dp})^2}}} \right. \\
 & - \sqrt{\left(1 - \frac{2\delta\Psi}{M^2 + 3\delta\sigma_{dp}}\right) + \sqrt{\left(1 - \frac{2\delta\Psi}{M^2 + 3\delta\sigma_{dp}}\right)^2 - \frac{12\delta\sigma_{dp}M^2}{(M^2 + 3\delta\sigma_{dp})^2}}} \\
 & + \frac{2\sqrt{2}\sigma_{dp}\mu_{dp}M^3}{(\sqrt{M^2 + 3\delta\sigma_{dp}}\delta)^3} \left[\left(\sqrt{1 + \sqrt{1 - \frac{12\delta\sigma_{dp}M^2}{(M^2 + 3\delta\sigma_{dp})^2}}} \right)^{-3} \right. \\
 & \left. - \left(\sqrt{\left(1 - \frac{2\delta\Psi}{M^2 + 3\delta\sigma_{dp}}\right) + \sqrt{\left(1 - \frac{2\delta\Psi}{M^2 + 3\delta\sigma_{dp}}\right)^2 - \frac{12\delta\sigma_{dp}M^2}{(M^2 + 3\delta\sigma_{dp})^2}}} \right)^{-3} \right] \\
 & - \frac{\mu_e}{\sigma} [\exp(\sigma\Psi) - 1] + \mu_i [1 + 3\beta - (1 + 3\beta + 3\beta\Psi + \beta\Psi^2)\exp(-\Psi)]. \tag{21}
 \end{aligned}$$

We can neglect non-thermal effects of the ions by simply setting $\alpha = 0$, in which case, our expression (21) is in agreement with Eq. (32) in Ref. 16.

The solitary wave solutions of Eq. (20) exist if (i) $(d^2V(\Psi)/d\Psi^2)_{\Psi=0} < 0$ so that a maximum occurs at the origin (the fixed point at the origin is unstable), (ii) $V(\Psi) < 0$ when $0 < \Psi < \Psi_{\max}$ for positive potential solitary waves and $\Psi_{\min} < \Psi < 0$ for negative potential solitary waves where $\Psi_{\max(\min)}$ is the maximum (minimum) value of Ψ for which $V(\Psi) = 0$, and (iii) $(d^3V(\Psi)/d\Psi^3)_{\Psi=0} > 0 (< 0)$ for positive (negative) potential solitary waves. In addition to the local maximum condition having to be satisfied at the origin (i), one requires $V(\Psi = \Psi_m) = 0$, $(dV(\Psi)/d\Psi)_{\Psi=\Psi_m} = 0$, and $(d^2V(\Psi)/d\Psi^2)_{\Psi=\Psi_m} < 0$ such that $V(\Psi) < 0$ for $0 < |\Psi| < |\Psi_m|$ for negative or positive potential double layer solutions.

In the limit of small solitary wave amplitude, we can expand $V(\Psi)$ about $\Psi = 0$ to third order to obtain

$$V(\Psi) = C_2\Psi^2 + C_3\Psi^3, \tag{22}$$

where

$$\begin{aligned}
 C_2 = & \frac{1}{2}(d^2V(\Psi)/d\Psi^2)_{\Psi=0} \\
 = & -\frac{1}{2} \left[\mu_i(1 - \beta) + \mu_e\sigma - \frac{1}{M^2} \left(1 + \frac{\delta\mu_{dp}}{1 - (3\delta\sigma_{dp}/M^2)} \right) \right] \tag{23}
 \end{aligned}$$

and

$$M_{\text{crit}} = \left\{ \frac{1 + \mu_{dp}\delta + 3\delta\sigma_{dp}[\mu_i - \mu_i\beta + \mu_e\sigma]}{2(\mu_i - \mu_i\beta + \mu_e\sigma)} + \frac{1 + \mu_{dp}\delta + 3\delta\sigma_{dp}[\mu_i - \mu_i\beta + \mu_e\sigma]}{2(\mu_i - \mu_i\beta + \mu_e\sigma)} \sqrt{1 - \frac{12\delta\sigma_{dp}(\mu_i - \mu_i\beta + \mu_e\sigma)}{[1 + \mu_{dp}\delta + 3\delta\sigma_{dp}(\mu_i - \mu_i\beta + \mu_e\sigma)]^2}} \right\}^{1/2}. \tag{26}$$

Whilst the expression (26) provides a lower limit on the range of Mach numbers for solitary waves to exist, upper

$$\begin{aligned}
 C_3 = & \frac{1}{6}(d^3V(\Psi)/d\Psi^3)_{\Psi=0} \\
 = & \frac{1}{6} \left[\mu_i - \mu_e\sigma^2 - \frac{3}{M^4} \left(1 - \delta^2\mu_{dp} \frac{(1 + (\delta\sigma_{dp}/M^2))}{[1 - (3\delta\sigma_{dp}/M^2)]^3} \right) \right]. \tag{24}
 \end{aligned}$$

We point out that in the absence of non-thermal ion effects ($\beta = 0$) our derived expressions (23) and (24) revert to the expressions (34) and (35) in Ref. 16.

The solution of Eq. (20) with $V(\Psi)$ given by Eq. (22) in the limit of small wave amplitude is given in Ref. 16 as

$$\Psi = \left(-\frac{C_2}{C_3} \right) \text{sech}^2 \left(\sqrt{\frac{-C_2}{2}} \xi \right). \tag{25}$$

If we closely examine Eq. (25), we can conclude that for $C_2 < 0$ (local maximum condition at origin) that small amplitude positive (negative) potential solitary wave solutions occur if $C_3 > 0$ ($C_3 < 0$).

In order for the local maximum condition to be satisfied at the origin ($\Psi = 0$), viz., $C_2 < 0$, where C_2 is given by Eq. (23), this establishes that the critical Mach number value must be exceeded for solitary wave solutions to be possible, i.e., $M > M_{\text{crit}}$ where M_{crit} which satisfies $C_2 = 0$ is given by the expression

Mach number limitations also occur for solitons, and justification for why these should occur is discussed in Sec. III.

III. REASONS WHY UPPER MACH NUMBER LIMITS EXIST FOR DA SOLITONS AND SUPERSOLITONS

Considering first why upper bounds arise on the Mach number ranges supporting positive potential solitons, it is clear from the expression for the number density of the adiabatic positive dust (18) that there exists a limiting value of Ψ , viz., $\Psi_{\max/\text{adiabatic}} = \frac{M^2 + 3\delta\sigma_{dp}}{2\delta} - \frac{\sqrt{12\delta\sigma_{dp}M^2}}{2\delta}$ such that if Ψ exceeds $\Psi_{\max/\text{adiabatic}}$ then Eq. (18) is no longer real valued.

For values of the Mach number which exceed the critical value (26), positive potential solitons will get stronger (amplitude will increase) with increasing values of the Mach number. This will not occur indefinitely but will terminate once $\Psi_{\max/\text{adiabatic}}$ is reached. The upper M limit for positive potential solitons which coincides with the limiting value of the potential $\Psi_{\max/\text{adiabatic}}$ is obtained by solving $V(\Psi = \Psi_{\max/\text{adiabatic}}) = 0$. If this upper limiting value of M is exceeded then Eq. (18) becomes complex valued because $\Psi > \Psi_{\max/\text{adiabatic}}$, in which case, $V(\Psi)$ will no longer have a positive root, and solitons having positive potentials are no longer possible. Similarly, if the positive dust pressure is neglected ($\sigma_{dp} = 0$), then the limiting value for positive values of the potential is given by $\Psi_{\max/\text{cold}} = M^2/2\delta$, which now corresponds to infinite compression in the number density of the positive dust (19). In this case, the upper M value where the existence of positive potential solitons terminates satisfies $V(\Psi = \Psi_{\max/\text{cold}}) = 0$.

Focusing now on the negative potential soliton structures, these will get stronger (the amplitude becomes increasingly negative) with increasing values of the Mach number but their existence terminates once the upper limit on M is reached which coincides with the minimum permitted value of the potential, viz., $\Psi_{\min/\text{cold}} = -M^2/2$ corresponding to infinite compression in the number density of the negative dust (17). This upper limit on the Mach number which restricts the occurrence of negative potential solitons satisfies $V(\Psi = \Psi_{\min/\text{cold}}) = 0$.

Besides the upper Mach number limitations which arise because the number densities of the inertial species have to remain real valued, there is another possibility that the upper M limit for negative (positive) potential solitons arises when a negative (positive) potential double layer occurs. The existence of a negative (positive) potential double layer requires that a negative (positive) root of $V(\Psi)$ must coincide with the presence of a local maximum ($d^2V(\Psi)/d\Psi^2 < 0$) at the position of the negative (positive) root.

There are also sometimes more complicated situations where solitary waves occur beyond the Mach number value for which a double layer is supported. This could signal the start of the Mach number range supporting supersolitons^{13,14} for which the existence of a double layer can provide a lower M bound. The other possibility for the existence of supersolitons is that the occurrence of three local extrema between the undisturbed conditions and the soliton amplitude in the Sagdeev potential signals the start of the range of Mach numbers supporting supersolitons. The existence of these supersolitons could then terminate when two of the extrema coalesce,¹³ in which case the occurrence of regular solitons

is supported, which ultimately terminates when the appropriate number density limit sets in. Alternatively, supersolitons can survive up to the M value where the number density limit sets in as is clearly demonstrated in our Figure 5 shown later.

IV. RESULTS AND DISCUSSION

We initially investigate the admissible dust-acoustic soliton Mach number ranges as a function of $\delta (= Z_{dp}m_{dn}/Z_{dn}m_{dp})$ which is the ratio of the charge-to-mass ratios of the positive to the negative dust. The solid curve (—) in Figure 1 which was generated using the expression (26) represents the lower limit on the Mach number, viz., $M_{\text{crit}}(\delta)$, which must be exceeded for solitons to occur. The existence of negative potential solitons (NPSs) starts at the value of M which lies just above the lower limiting curve denoted by (—). These become stronger (the potential becomes increasingly negative) with increasing values of the Mach number. This does not occur indefinitely, but the existence of NPSs terminates once the upper limit on M is encountered which coincides with a point on (· · ·) in Figure 1. The upper M limit for NPSs coincides with the limiting value of the negative potential, viz., $\Psi_{\min/\text{cold}} = -M^2/2$ such that Eq. (17) is no longer real valued for $\Psi < \Psi_{\min/\text{cold}}$. The values for the upper M limits on (· · ·) were obtained numerically by solving $V(\Psi_{\min/\text{cold}}) = 0$. The existence of dust-acoustic solitons having positive potentials (PPSs) only starts at the value $\delta = 1.67$. These (PPSs) also become stronger with increasing M , but they will cease to exist once the value for M which lies on (- -) is reached. The upper limiting value of the Mach number, where the existence of PPSs terminates coincides with the limiting value of the potential (positive), viz.,

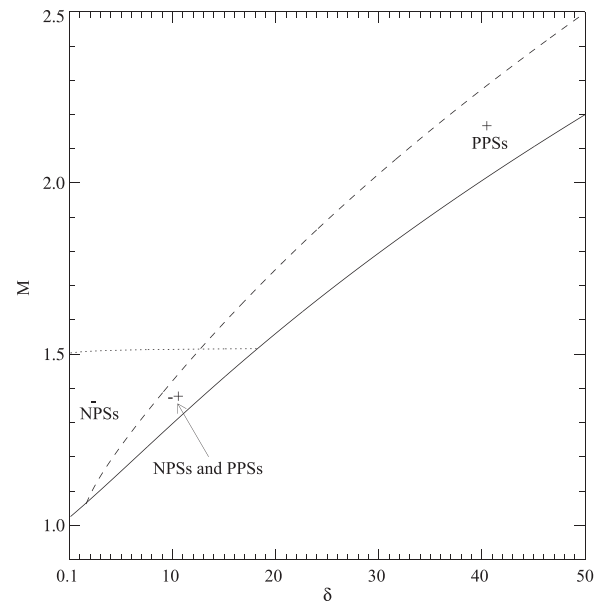


FIG. 1. The existence regimes of solitary waves as a function of δ where the curves correspond to the critical Mach number (—), negative dust compression limit (· · ·), and the upper Mach number limit for PPSs, beyond which the adiabatic positive dust number density (18) becomes complex valued (- -). The “+” indicates regions where only PPSs occur, “-+” indicates regions where both NPSs and PPSs coexist, and “-” denotes regions where only NPSs occur. The fixed parameters are $\sigma_{dp} = 0.01$, $\alpha = 0.1$, $\sigma = T_i/T_e = 0.5$, $\mu_e = 0.25$, $\mu_i = 1.2$, and $\mu_{dp} = 1 + \mu_e - \mu_i = 0.05$.

$\Psi_{\text{max/adiabatic}} = \frac{(M^2 + 3\delta\sigma_{dp}) - \sqrt{12\delta\sigma_{dp}M^2}}{2\delta}$ such that Eq. (18) becomes complex valued when $\Psi > \Psi_{\text{max/adiabatic}}$. The upper Mach number limiting curve for PPSs which is shown as (- -) in Figure 1 was generated by numerically solving $V(\Psi_{\text{max/adiabatic}}) = 0$ as a function of δ . Having identified the minimum and maximum values of the Mach number for which NPSs and PPSs are supported, three different existence regions for large amplitude dust-acoustic solitons are depicted in Figure 1, viz., the region marked (-) denotes where only NPSs occur, the region marked (+) denotes where the existence of only PPSs is supported, whereas both NPSs and PPSs coexist (are simultaneously supported) in the overlap region marked (-+) which is common to both the regions marked (-) and (+). It is seen in Figure 1 that the existence of NPSs is supported for small δ values but terminates at $\delta = 18.23$. The existence of PPSs only starts at $\delta = 1.67$ and coexistence of NPSs and PPSs occurs for $1.67 \leq \delta \leq 18.23$.

Choosing the value $\delta = 10$ which coincides with the region in parameter space where NPSs and PPSs were seen to coexist marked (-+) in Figure 1, we now focus on the effect of positive dust temperature on the existence of dust-acoustic solitons. The lower limiting values of the Mach number which have to be exceeded for DA solitons to occur coincide with points on the curve denoted by (-) in Figure 2. The upper M limits for NPSs coincide with M values which lie on ($\cdot \cdot \cdot$) in Figure 2 whereas the existence of PPSs terminates at the M values which lie on the curve denoted by (- -) in Figure 2. It is seen in Figure 2 that the admissible DA soliton Mach number ranges supporting the existence of PPSs is widest when the positive dust is cold ($\sigma_{dp} = 0$), but the permitted M ranges are seen to narrow quite considerably when

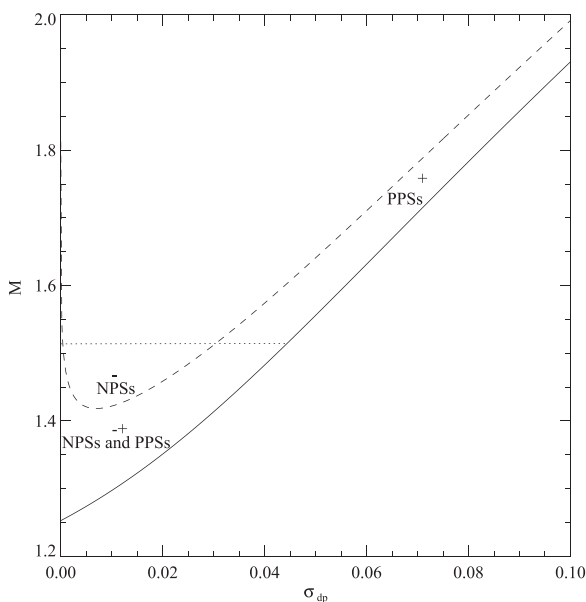


FIG. 2. The existence regimes of solitary waves as a function of the positive dust temperature σ_{dp} . The curves correspond to the critical Mach number (-), negative dust compression limit ($\cdot \cdot \cdot$), and the upper Mach number limit for PPSs (- -). The “+” indicates regions where only PPSs occur, “-+” indicates regions where both NPSs and PPSs coexist, and “-” denotes regions where only NPSs occur. The fixed parameters are $\delta = 10$, $\alpha = 0.1$, $\sigma = T_i/T_e = 0.5$, $\mu_e = 0.25$, $\mu_i = 1.2$, and $\mu_{dp} = 1 + \mu_e - \mu_i = 0.05$.

the pressure of the positive dust species is retained ($\sigma_{dp} > 0$). Whilst both NPSs and PPSs are seen to be supported for small values of the positive dust pressure or when the positive dust is cold ($\sigma_{dp} = 0$), only PPSs are seen to be supported for $\sigma_{dp} > 0.0443$. This shows the importance of including dust pressure in the theoretical model of the DA solitons. This does not justify the claim that dust pressure can be neglected.¹⁵

Next, we investigate the DA soliton existence regions as a function of the ion non-thermal parameter (α) for three different fixed values for δ , viz., where the charge-to-mass ratio of the positive dust is less than ($\delta = 0.1$), comparable to ($\delta = 1$) and greater than ($\delta = 10$) the charge-to-mass ratio of the negative dust. In presenting our results, we terminate the existence regions in Figures 3, 4, and 7 at the value $\alpha = 0.45$ for the ion non-thermal parameter corresponding to $\beta \approx 0.77$, which may still be considered to be quite high.¹¹ Figure 3(a) depicts the Mach number ranges supporting DA solitons for $\delta = 0.1$ for a finite value of the temperature of the positive dust ($\sigma_{dp} = 0.01$). The critical values of M lie on lower limiting curve (-) in Figure 3(a). Upper limiting values of M for NPSs coincide with points which lie on ($\cdot \cdot \cdot$). The upper M limits for PPSs which lie on the curve (- -) are not M values, beyond which the positive dust number density (18) ceases to be real valued, but these are values for M for which positive potential double layers occur. NPSs are seen to be supported for $0 \leq \alpha \leq 0.4314$,

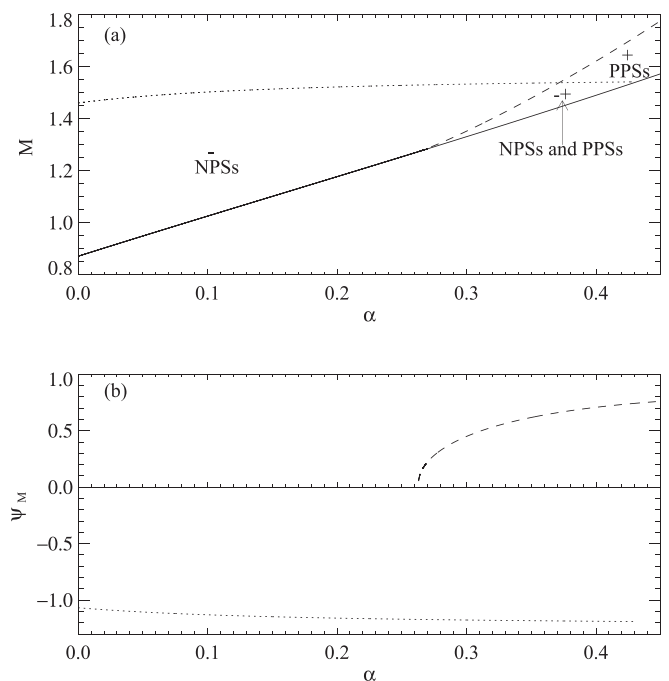


FIG. 3. (a) The existence regimes of solitary waves as a function of the ion non-thermal parameter α . The curves correspond to the critical Mach number (-), negative dust compression limit ($\cdot \cdot \cdot$), and the upper Mach number limit for PPSs which yields double layers (- -). (b) Variation of limiting values of the negative potential ($\cdot \cdot \cdot$) and maximal positive potential double layer amplitudes (- -) with the ion non-thermal parameter α . The fixed parameters are $\delta = 0.1$, $\sigma_{dp} = 0.01$, $\sigma = T_i/T_e = 0.5$, $\mu_e = 0.25$, $\mu_i = 1.2$, and $\mu_{dp} = 1 + \mu_e - \mu_i = 0.05$.

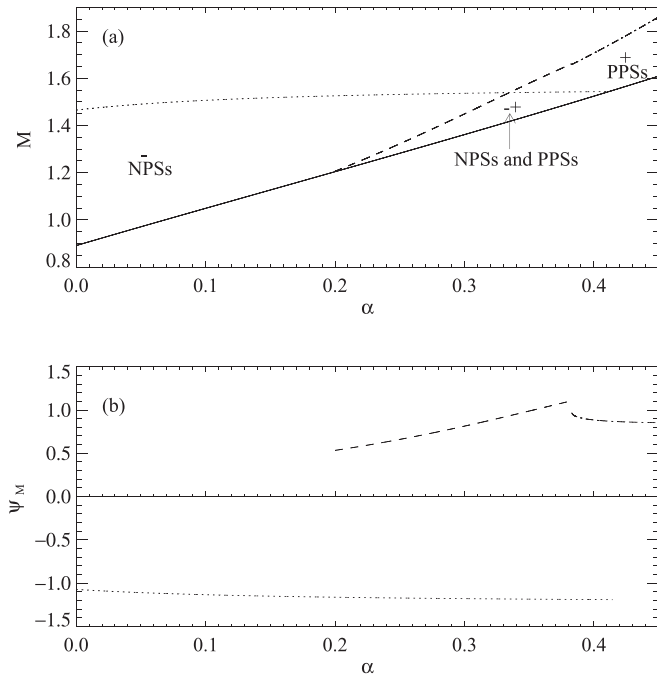


FIG. 4. (a) The existence regimes of solitary waves as a function of the ion non-thermal parameter α . The curves correspond to the critical Mach number (—), negative dust compression limit (\cdots), and upper Mach number limit for PPSs, beyond which the adiabatic positive dust number density (18) becomes complex valued (---) and positive double layers occur (— · —). (b) Variation of the limiting values of the negative (\cdots) and positive (---) potential and maximal positive potential double layer amplitudes (— · —) with the ion non-thermal parameter α . The fixed parameters are $\delta = 1$, $\sigma_{dp} = 0.01$, $\sigma = T_i/T_e = 0.5$, $\mu_e = 0.25$, $\mu_i = 1.2$, and $\mu_{dp} = 1 + \mu_e - \mu_i = 0.05$.

which not only includes finite values of α for which the ions are non-thermal but also includes the value ($\alpha = 0$) corresponding to Boltzmann distributed ions. On the other hand, non-thermal effects of the ions is found to be crucial for the

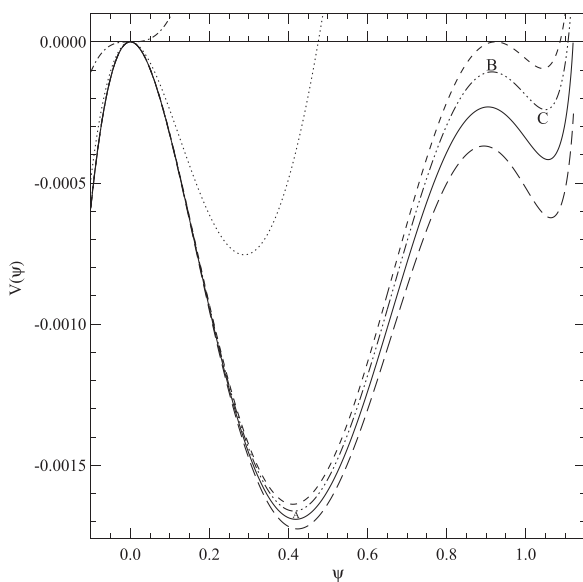


FIG. 5. The Sagdeev potential as a function of Ψ . The curves correspond to $M = 1.5016958$ (— · —), $M = 1.63$ (\cdots), $M = 1.66821887452588$ (---), $M = 1.669$ (— · · —), $M = 1.669324685$ (—), and $M = 1.671$ (— —). The fixed parameters are $\delta = Z_{dp}m_{dn}/Z_{dn}m_{dp} = 1$, $\alpha = 0.3865$, $\sigma = T_i/T_e = 0.5$, $\mu_e = 0.25$, $\mu_i = 1.2$, $\mu_{dp} = 1 + \mu_e - \mu_i = 0.05$, and $\sigma_{dp} = 0.01$.

existence of PPSs since these only occur for finite values for α , viz., $\alpha > 0.263042$, as seen in Figure 3(a). Although both polarities of solitons are possible in the coexistence region marked (-+) for $0.263042 \leq \alpha \leq 0.4314$, only PPSs occur for $\alpha > 0.4314$ in the region marked (+) in Figure 3(a) when the deviation of the ions from a thermal Maxwellian distribution is large. In Figure 3(b) limiting values of the negative potentials (\cdots), viz., $\Psi_{\min/cold} = -M^2/2$, and maximal positive potential double layer amplitudes (---) are shown which correspond to the respective upper M limits for NPSs and PPSs in Figure 3(a).

Moving now to the higher value $\delta = 1$, the admissible soliton Mach number ranges in Figure 4(a) look quite similar to those shown in Figure 3(a); however, there is a difference. Two different regions in parameter space which support PPSs have been identified in Figure 4(a), and the reasons for the upper Mach number limitations are different for these two regions. Non-thermal effects of the ions again is crucial for the existence of PPSs for this particular value of δ , viz., $\delta = 1$. The existence of PPSs which starts at $\alpha = 0.1972$ and ends at $\alpha = 0.38285$, denoted by (---) in Figure 4(a), are limited by the adiabatic positive dust number density (18) becoming complex valued. The second region in parameter space corresponding to $\alpha > 0.38285$ in Figure 4(a) also supports the existence of PPSs, but these are now limited by the occurrence of positive potential double layers for M values which lie on the upper limiting curve (— · —). Limiting values of the negative potential (\cdots), the positive potential (---), and the maximal positive potential double layer amplitudes (— · —) are shown in Figure 4(b).

It is important to mention that although double layer M values (— · —) are shown as upper M limits in Figure 4(a) for values of the ion non-thermal parameter spanning

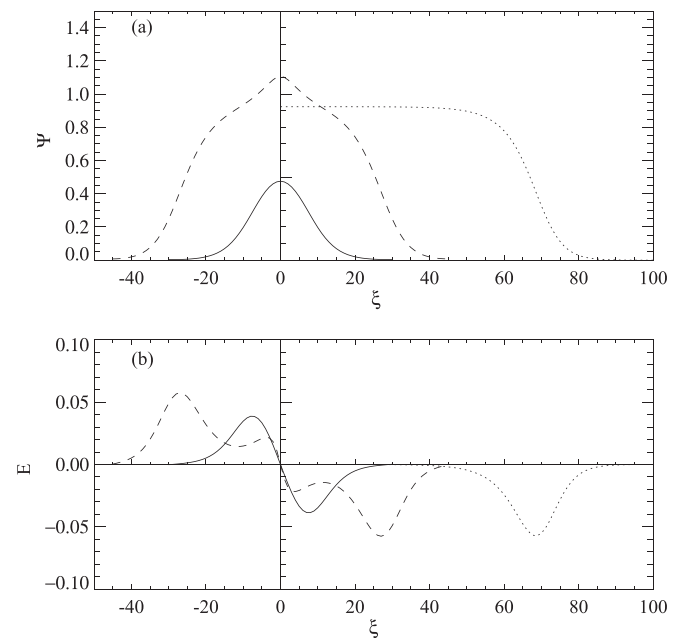


FIG. 6. (a) Potential and (b) electric field profiles as a function of ξ . The curves correspond to $M = 1.63$ (—), $M = 1.66821887452588$ (\cdots), and $M = 1.669$ (---). The fixed parameters are $\delta = Z_{dp}m_{dn}/Z_{dn}m_{dp} = 1$, $\alpha = 0.3865$, $\sigma = T_i/T_e = 0.5$, $\mu_e = 0.25$, $\mu_i = 1.2$, $\mu_{dp} = 1 + \mu_e - \mu_i = 0.05$, and $\sigma_{dp} = 0.01$.

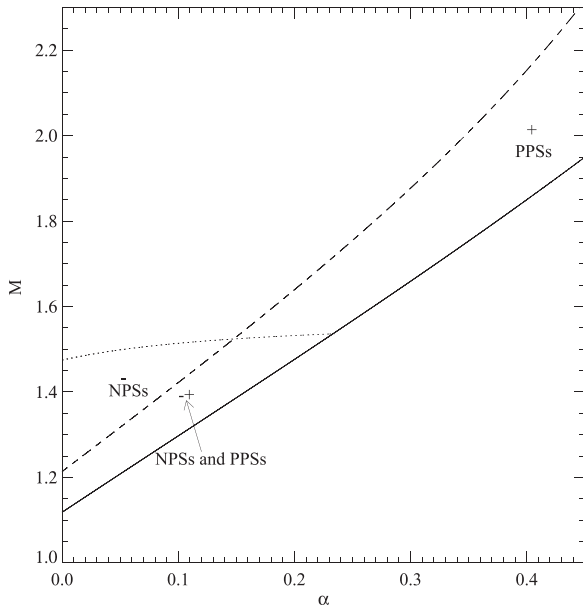


FIG. 7. The existence regimes of solitary waves as a function of the ion non-thermal parameter α . The curves correspond to the critical Mach number (—), negative dust compression limit (\cdots), and upper Mach number limit for PPSs, beyond which the adiabatic positive dust number density (18) becomes complex valued (— · —). The fixed parameters are $\delta = 10$, $\sigma_{dp} = 0.01$, $\sigma = T_i/T_e = 0.5$, $\mu_e = 0.25$, $\mu_i = 1.2$, and $\mu_{dp} = 1 + \mu_e - \mu_i = 0.05$.

$0.38286 \leq \alpha \leq 0.3907$, positive potential solitons are still found to occur beyond the M values shown for double layers. These are precisely the supersolitons.^{13,14} This point is clearly illustrated in Figure 5 which depicts Sagdeev potentials for different values of the Mach number. For the fixed value $\alpha = 0.3865$, we observe that a soliton occurs for $M = 1.63$ (\cdots) which exceeds the critical value $M = 1.5016958$ ($-\cdot-$). A double layer is seen to occur for a higher value of $M = 1.66821887452588$ ($-$), but the existence of PPSs does not terminate here because a supersoliton is still seen to occur for a higher Mach number than the double layer, viz., $M = 1.669$ ($-\cdot\cdot-$). The shape of the Sagdeev potential for $M = 1.669$ ($-\cdot\cdot-$) is precisely the same as for a supersoliton^{13,14} which has three local extrema labelled A, B, and C between $\Psi = 0$ and the amplitude Ψ_M of the nonlinear structure. In comparison, the Sagdeev potential for an ordinary soliton for $M = 1.63$ (\cdots) has only one local extremum between $\Psi = 0$ and Ψ_M . We observe that the double layer $M = 1.66821887452588$ value provides a lower M limit on the range of Mach number values supporting supersolitons in Figure 5. We consider now what limits the existence of the positive potential structures in Figure 5 from the high Mach number side. One of the possibilities for the existence of an upper M limit where the existence of the positive potential supersolitons shown in Figure 5 ceases is when A and B coalesce.¹³ We can infer from Figure 5 that the local extrema such as those labelled A, B, and C in the Sagdeev potential corresponding to $M = 1.669$ (for higher M values labelling is not shown) will remain distinct in the structures starting from $M = 1.66821887452588$ up to the upper M limit. The extrema labelled B and C will not coalesce because of the presence of the positive double layer, neither do A and B coalesce, viz., supersolitons are seen to occur in Figure 5 for Mach number

values which exceed that for the double layer and go right up to the upper $M = 1.6699324685$ limit which is imposed by the constraint that the number density of the adiabatic positive dust (18) must remain real valued. The upper M limits beyond which the adiabatic dust number density (18) is no longer real valued are not shown for α values in the range $0.38286 \leq \alpha \leq 0.3907$ in Figure 4(a) since these are so close in magnitude to the double layer M values ($-\cdot\cdot-$) indicated in the figure to the extent that these are not distinguishable from the double layer Mach number values.

To illustrate the difference between an ordinary soliton and a supersoliton more clearly, we show the potential (Figure 6(a)) and electric field profiles (Figure 6(b)) for a soliton ($M = 1.63$, — solid curve), a double layer ($M = 1.66821887452588$, $-\cdot\cdot-$ curve), and a supersoliton ($M = 1.669$, — · — curve). It is clear that the profiles for the supersolitons are distorted because of the presence of subsidiary extrema as compared to the ordinary solitons or double layer. Also, the observation in Figure 6(b) that the first peak is higher than the second peak in the electric field (E) signature for the supersoliton ($-\cdot\cdot-$) because the local minimum labelled A is deeper than that labelled C for the supersoliton ($-\cdot\cdot-$) shown for $M = 1.669$ in Figure 5 is consistent with what is mentioned in Ref. 14. Had the local minimum C been deeper than A in the Sagdeev potential for the supersoliton ($-\cdot\cdot-$) in Figure 5, then the second peak in the corresponding electric field profile (E) would have been higher than the first peak. For higher values of the ion non-thermal parameter which exceed $\alpha = 0.3907$, only solitons are found which do not occur beyond the M values ($-\cdot\cdot-$) shown for double layers in Figure 4(a).

The DA soliton existence domains for $\delta = 10$ are depicted in Figure 7. Contrary to our findings for $\delta = 0.1$ (Figure 3(a)) and $\delta = 1$ (Figure 4(a)) we observe in Figure 7 ($\delta = 10$) that PPSs are not only supported for finite values of α when non-thermal effects of the ions are included, but PPSs also occur when the ions in the model are Boltzmann distributed ($\alpha = 0$). The upper M limits ($-$) for PPSs in Figure 7 are imposed by the adiabatic positive dust number density (18) becoming complex valued. Although non-thermal effects of the ions are crucial for the existence of PPSs such as for $\delta = 0.1$ (Figure 3(a)) and $\delta = 1$ (Figure 4(a)) but not found to be essential for existence of PPSs such as for $\delta = 10$ (Figure 7). The Mach number ranges for PPSs are sensitive to the deviation of the ions from a thermal Maxwellian distribution and are seen to widen quite significantly for increasing values of α .

V. CONCLUSIONS

We have investigated the existence of large amplitude dust-acoustic solitons and supersolitons for the model composed of Boltzmann electrons, cold negative dust, adiabatic positive dust, and non-thermal ions. We encountered a region in parameter space where positive potential dust-acoustic supersolitons are supported for ion non-thermal parameter values lying in the range $0.38286 \leq \alpha \leq 0.3907$ for the fixed $\delta = 1$ value. The occurrence of double layers in this region of parameter space signalled the start of the range of Mach numbers for which supersolitons are supported, but

the existence of these, ultimately, terminated when the adiabatic dust number density limit set in. It is shown that the electric field signatures of supersolitons differ from those of regular solitons in that they appear distorted because of the presence of subsidiary extrema in the wings of the bipolar electric field structures. This will have implications for satellite observations of nonlinear wave structures in space plasmas since it will be easy to distinguish between a supersoliton and a regular soliton from the measured electric field signatures of the nonlinear structures. Beyond $\alpha = 0.3907$, solitons were not found beyond the M values imposed by the occurrence of positive potential double layers.

The existence regions for PPSs were found to be very sensitive to the magnitude of the ratio of the charge-to-mass ratios of the positive to negative dust, δ . Only NPSs were found for small δ values which are less than $\delta = 1.67$, and these are limited by infinite compression in the number density of the negative dust. The existence of positive potential solitons only starts at the value $\delta = 1.67$, and these terminate at the upper limiting values of M which are imposed by the constraint that the adiabatic positive dust number density has to remain real valued. The coexistence of NPSs and PPSs was found to be supported for α values in the range $1.67 \leq \delta \leq 18.23$, but beyond this range only PPSs occur.

Non-thermal effects of the ions was found to be crucial for the existence of PPSs for $\delta = 0.1$ and $\delta = 1$ as can be inferred from plots which show the DA soliton existence regions as a function of α . For $\delta = 0.1$ the upper M limits for PPSs coincide with the occurrence of positive potential double layers. Although the PPSs existence regions for $\delta = 1$ look quite similar to those found for $\delta = 0.1$, there is a range of α values where the adiabatic dust density limit restricts PPSs, but this is then followed by the region in parameter space where positive potential double layers limit the occurrence of PPSs.

For higher values of δ , say, $\delta = 10$, the existence of PPSs is supported by both a non-thermal ion velocity distribution ($\alpha > 0$) as well as a Boltzmann distribution for the ions ($\alpha = 0$). The range of Mach numbers supporting PPSs is widest when the positive dust is assumed to be cold ($\sigma_{dp} = 0$) but is found to narrow considerably when positive dust pressure is included. The upper M limit for PPSs when the positive dust is cold (warm) corresponding to $\sigma_{dp} = 0$ ($\sigma_{dp} > 0$) coincides with the limiting value of the

potential beyond which the number density of the cold (adiabatic) positive dust is no longer real valued. The coexistence of NPSs and PPSs is supported if the positive dust is cold ($\sigma_{dp} = 0$) or for small values of the positive dust temperature, because only PPSs are possible if $\sigma_{dp} > 0.0443$.

In general, for all three values for δ which we considered in this study, viz., $\delta = 0.1, 1$, and 10 , the Mach number ranges supporting PPSs are seen to widen for increasing deviations of the ions from a thermal Maxwellian velocity distribution (increasing α).

ACKNOWLEDGMENTS

S.K.M., R.B., and S.V.S. would like to thank NRF South Africa and Department of Science and Technology, New Delhi, India, respectively, for the financial support. The work was performed under the Indo-South Africa Bilateral Project "Linear and nonlinear studies of fluctuation phenomena in space and astrophysical plasmas." G.S.L. thanks the National Academy of Sciences, India for the support under the NASI-Senior Scientist Platinum Jubilee Fellowship.

¹A. A. Mamun, *Astrophys. Space Sci.* **268**, 443 (1999).

²A. A. Mamun, *Phys. Lett. A* **372**, 686 (2008).

³A. A. Mamun, *Phys. Lett. A* **372**, 884 (2008).

⁴R. A. Cairns, A. A. Mamun, R. Bingham, R. Boström, R. O. Dendy, C. M. C. Nairn, and P. K. Shukla, *Geophys. Res. Lett.* **22**, 2709, doi:10.1029/95GL02781 (1995).

⁵A. A. Mamun, R. A. Cairns, and P. K. Shukla, *Phys. Plasmas* **3**, 2610 (1996).

⁶C. A. Mendoza-Briceño, S. M. Russell, and A. A. Mamun, *Planet. Space Sci.* **48**, 599 (2000).

⁷S. K. Maharaj, S. R. Pillay, R. Bharuthram, S. V. Singh, and G. S. Lakhina, *Phys. Scr.* **T113**, 135 (2004).

⁸S. K. Maharaj, S. R. Pillay, R. Bharuthram, R. V. Reddy, S. V. Singh, and G. S. Lakhina, *J. Plasma Phys.* **72**, 43 (2006).

⁹F. Verheest and S. R. Pillay, *Phys. Plasmas* **15**, 013703 (2008).

¹⁰F. Verheest and S. R. Pillay, *Nonlinear Processes Geophys.* **15**, 551 (2008).

¹¹F. Verheest, *Phys. Plasmas* **16**, 013704 (2009).

¹²T. K. Baluku, M. A. Hellberg, and F. Verheest, *Europhys. Lett.* **91**, 15001 (2010).

¹³F. Verheest, M. A. Hellberg, and I. Kourakis, *Phys. Plasmas* **20**, 012302 (2013).

¹⁴F. Verheest, M. A. Hellberg, and I. Kourakis, *Phys. Rev. E* **87**, 043107 (2013).

¹⁵F. Verheest, *Phys. Plasmas* **18**, 083701 (2011).

¹⁶A. A. Mamun, *Phys. Rev. E* **77**, 026406 (2008).

¹⁷S. K. Maharaj, R. Bharuthram, S. V. Singh, S. R. Pillay, and G. S. Lakhina, *J. Plasma Phys.* **76**, 441 (2010).